J. Anat. (2006) **208**, pp3–12

Morphological characterization of GFP stably transfected adult mesenchymal bone marrow stem cells

Stefania Raimondo,* Claudia Penna,* Pasquale Pagliaro and Stefano Geuna

Department of Clinical and Biological Sciences, University of Turin, Orbassano (TO), Italy

Abstract

Increasing attention is being given to the use of adult rather than embryonic stem cells, both for research and for the development of transplantation treatments for human disease. In particular, mesenchymal bone marrow stem cells have been studied extensively because of their ability to self-renew and to give rise to various differentiated cell types, and because of the relative ease with which they can be obtained and cultured. In addition, the possibility of labelling stem cells with green fluorescent protein before transplantation has opened new and promising perspectives for their use in basic research. Because no structural or ultrastructural description of adult mesenchymal stem cells is available in the literature, this paper describes their morphology as revealed by light, confocal and electron microscopy, focusing on cells that are particularly suitable for transplantation studies, i.e. those derived from rat bone marrow transfected with green fluorescent protein. The results provide a basis for experimental studies of the differentiation of these cells in normal and pathological tissues.

Key words cell transplantation; confocal microscopy; electron microscopy; rat.

Introduction

Stem cells are defined by their ability to self-renew and to form one or more differentiated cell types (Geuna et al. 2001; Lovell & Mathur, 2004). Because stem cells are the precursors of many tissues, and thus have the potential to generate replacement tissue for damaged organs, they are good candidates for transplantation in the treatment of such human conditions as Parkinson's disease (Dunnett et al. 2001), diabetes (Henningson et al. 2003) and heart disease (Orlic et al. 2001, 2002; Herzog et al. 2003; Eisenberg & Eisenberg, 2004).

Embryonic stem cells (Gerecht-nir et al. 2004) are distinguished from those found in adult somatic tissue, known as adult stem cells (Geuna et al. 2001; Abbott & Giordano, 2003; Young & Black, 2004). For transplantation purposes, adult stem cells have advantages over embryonic stem cells. They can be obtained from the patient's own cells, expanded in culture and then re-introduced into the same patient, thus avoiding some of the problems of allotransplantation of embryonic stem cells, especially ethical restrictions (Hassink et al. 2003).

A well-known type of adult stem cells are bone marrow mesenchymal (stromal) stem cells (MSCs). MSCs were first described by Friedenstein et al. (1974), 10 years after the characterization of haematopoietic stem cells (Lewis & Trobaugh, 1964). MSCs maintain an undifferentiated and stable phenotype over many generations *in vitro* and are progenitors for different types of somatic cells, such as osteocytes, chondrocytes and adipocytes (Pittenger et al. 1999; Javazon et al. 2001; Barry & Murphy, 2004).

MSCs adhere to the tissue culture substrate and, if primary cultures are maintained for 12–14 days, the non-adherent haematopoietic stem cell fraction is depleted (Barry & Murphy, 2004). Although MSCs represent a very small fraction of the total population of nucleated cells in the marrow (Pittenger et al. 1999), they can be isolated and expanded with high efficiency (Orlic et al. 2002).

Although the growing interest in MSCs has led to a number of biochemical and immuncytochemical

Correspondence
Dr Stefano Geuna, Dipartimento di Scienze Cliniche e Biologiche, Università di Torino, Ospedale San Luigi, Regione Gonzole 10, 10043 – Orbassano (TO), Italy. T: +39 011 67 05 435; F: +39 011 90 38 639; E: stefano.geuna@unito.it

*The first two authors contributed equally to this work.

Accepted for publication *2 October 2005*

characterization studies (Young & Black, 2004), structural and ultrastructural descriptions of their phenotype are lacking. To fill this gap, the present study was aimed at providing an in-depth morphological description of adult cultured rat MSCs using light, confocal and electron microscopy. In addition, because many transplantation studies with MSCs use green fluorescent protein-(GFP-) positive cells so that they can be easily located in the receiving tissue, we focused on suspensions of GFP-positive MSCs because this is the condition in which these cells are transplanted into receiving tissues.

Materials and methods

Isolation of stem cells and cell cultures

To allow grafted cells to be identified in the recipient tissue, donor cells were obtained from transgenic rats overexpressing the enhanced green fluorescent protein under the control of the cytomegalovirus enhancer and the chicken β-actin promoter derived from an expression vector, pCAGGS (Okabe et al. 1997).

MSCs were harvested from femur and tibia bone marrow of GFP stably transfected adult rats (body weight 450–550 g) and adult control rats of the same weight. The rats were housed in identical cages and were allowed access to water and a standard rodent diet *ad libitum*. The animals received care in accordance with Italian law (DL-116, 27 January 1992), which complies with the Guide for the Care and Use of Laboratory Animals by the US National Research Council. In brief, animals were anaesthetized with urethane (1 g kg^{-1}, i.p.). MSCs were extracted by inserting a 21-gauge needle into the shaft of the bone and flushing it with 30 mL of complete α-modified Eagle's medium (αMEM) containing 20% fetal bovine serum (FBS), 2 mM L-glutamine, 100 U mL^{-1} penicillin and 100 μg mL^{-1} streptomycin. The cells were filtered through a 70-μm nylon filter (Falcon, Franklin Lakes, NJ, USA) and the cells from one rat were plated into one 75-cm^2 flask. They were grown in complete αMEM containing 10% FBS, 2 mM L-glutamine, 100 U mL^{-1} penicillin and 100 μg mL^{-1} streptomycin at 37 °C and 5% CO_2 for 3 days. The medium was then replaced with fresh medium and the adherent cells were grown to 90% confluence to obtain samples here defined as passage zero (P0) cells.

The P0 MSCs were washed with phosphate-buffered saline (PBS) and detached by incubation with 0.25% trypsin and 0.1% EDTA (Sigma, St Louis, MO, USA) for 5–10 min at 37 °C. Complete medium was added to inactivate the trypsin. The cells were centrifuged at 450***g*** for 10 min, resuspended in 1–10 mL complete medium, counted manually in duplicate using a Bürker's chamber, and plated as P1 on 58-cm^2 plates (Falcon) at densities of *c*. 2000 cells cm^2. Complete medium was replaced every 3–4 days over the 18- to 24-day period of culture (Friedenstein et al. 1976; Javazon et al. 2001).

To verify that the cell population that we are investigating comprises MSCs, a differentiation experiment was carried out by adding 1 μM dexamethasone, 1.7 μM insulin and 0.5 mM IBMX (isobutyl-methylxanthine) to culture medium for 5 days. Under these experimental conditions, it has been previously shown that MSCs differentiate into adipocytes (Rim et al. 2005).

Light, confocal and electron microscopy

Morphological analysis was carried out at P6 (18–24 days of culture). To investigate adherent MSCs, cells were cultured on Lab-Tek chamber slides (Sigma). To investigate MSCs in suspension, cells were detached from the Petri dish by incubation with 0.25% trypsin and 0.1% EDTA for 5–10 min at 37 °C. Complete medium was added to inactivate the trypsin and one drop of medium containing stem cells was put on a slide.

For imaging of the GFP autofluorescence of the MSCs, unstained slides were directly analysed by confocal laser microscopy. For light microscope observation, some slides were stained with haematoxylin and eosin. To confirm that our cultured cells were indeed stem cells, some slides were then incubated with primary antibody against CD90 (Thy-1.1 monoclonal, mouse, 1 : 50, BD Pharmingen, Milano, Italy) or against CD34 (monoclonal, mouse, 1 : 50, Santa Cruz Biotechnology, Santa Cruz, CA, USA). After washing in PBS, sections were then incubated with TRITC secondary antibody (anti-mouse IgG, Dako, Milan, Italy). For nuclear staining, some slides were incubated for 2 min with propidium iodide (Sigma). Finally, slides obtained from cells stimulated with dexamethasone were stained with Nile red (0.4 mg mL^{-1}; Sigma) for 5 min (Greenspan et al. 1985; Wezeman & Gong, 2004).

Confocal imaging was carried out with an LSM 510 confocal laser microscopy system (Zeiss, Jena, Germany), which incorporates two lasers (Ar and HeNe) and is equipped with an inverted Axiovert 100M microscope. Confocal fluorescence images were taken using a 20× Plan-NEOFLUAR objective [numerical aperture (NA) =

0.50] and a 40× Plan-NEOFLUAR objective (NA = 0.75). An electronic zoom with a magnification ranging from 1 to 8 was employed to obtain the magnifications indicated in the figures. To visualize GFP fluorescence, we used excitation from the 488-nm Ar laser line and emission passing through a band-pass (BP) 505–530 filter, which passes wavelengths of 505–530 nm to the detector. To visualize TRITC, propidium iodide and Nile red fluorescence, we used excitation from the 543-nm HeNe laser line and emission passing through a high-pass (LP) 560 filter, which passes wavelengths of greater than 560 nm to the detector. Images created with the BP 505–530 filter were digitally coloured green. Images created with the LP 560 filter were digitally coloured red.

For electron microscopy, MSCs were centrifuged at 900***g*** for 5 min and the pellet was fixed in 1% paraformaldehyde (Merck, Darmstadt, Germany), 1.25% glutaraldehyde (Fluka, St Louis, MO, USA) and 0.5% saccharose in 0.1 M Sörensen phosphate buffer (pH 7.2) for 2 h. The pellet was then washed in 1.5% saccharose in 0.1 M Sörensen phosphate buffer (pH 7.2) for 6–12 h, post-fixed in 2% osmium tetroxide, dehydrated and embedded in Glauert's embedding mixture, which consists of equal parts of Araldite M and Araldite Härter, HY 964 (Merck), supplemented with 2% of the accelerator DY 064 (Merck). The plasticizer dibutyl phthalate was added at 0.5%. Thin sections (70 nm) were cut using a Leica Ultracut UCT, stained with uranyl acetate and lead citrate, and examined in a JEM-1010 transmission electron microscope (JEOL, Tokyo, Japan) equipped with a Mega-View-III digital camera and a Soft-Imaging-System (SIS, Münster, Germany) for computerized acquisition of images.

Results

Figure 1 provides evidence that the cells that we isolated were MSCs. Specifically, Fig. 1(A–C) shows GFP-positive cells labelled with anti-CD90 antibody, a stem cell marker expressed by cultured MSCs (Pittenger et al. 1999; Kicic et al. 2003; Pittenger & Martin, 2004; Strawn et al. 2004; Young & Black, 2004; Muscari et al. 2005). The lack of anti-CD34 immunolabelling (images not shown) ruled out that the cells were of haematopoietic origin. The mesenchymal origin of the cells was further supported by Nile red staining (Greenspan et al. 1985; Wezeman & Gong, 2004) after culturing under adipocyte differentiation conditions (Rim et al. 2005) (Fig. 1D–F). In many cells, the presence of intracytoplasmic heavily stained lipid droplets points to the differentiation in adipocytes.

Figure 2(A) shows confocal imaging of suspended MSCs. Green autofluorescence was clear and intense throughout the cell body and cells had a size ranging from 10 to 20 μm. The nucleus, stained with propidium iodide, appeared eccentric and irregularly shaped. After haematoxylin and eosin staining (Fig. 2B–D), the MSCs showed a basophilic and eccentric nucleus and an eosinophilic cytoplasm in which two differently stained areas were clearly distinguishable: a more intensely stained inner zone and a thin, relatively pale peripheral zone (Fig. 2D). The plasma membrane showed an irregular profile. In adherent MSCs (Fig. 2E,F) green autofluorescence was more evident at nuclear level as the cytoplasm was more distended, indicating the presence of adhesion pseudopodia.

Electron microscopy (Figs 3–5) clarified the interpretation of the light and confocal laser microscope images. At low magnification (Fig. 3), all the MSCs appeared similar, with a pale, eccentric and irregularly shaped nucleus with one or more nucleoli located near the perinuclear cisternae (Fig. 4A–C). Chromatin was spread throughout the nucleus except for a thin dense layer located immediately inside the perinuclear cisternae (Figs 4B,D and 5A,F–H).

Ultrastructural observations clarified the two differently stained cytoplasmic areas revealed by light microscopy (Fig. 2D): the inner part of the cytoplasm was rich in organelles whereas the peripheral zone was not (Figs 4C,E and 5B). In particular, the inner cytoplasmic area was rich in round and elongated mitochondria (Figs 4D,F and 5C,D) with electron-dense matrices (Fig. 5C,D) and thick cristae (Fig. 5D). By contrast, the endoplasmic reticulum was detectable in both the inner and the peripheral cytoplasmic zones. It was mainly granular and organized into small elements (Figs 4A,B,D,G and 5C). Often, the endoplasmic reticulm was dilatated (Figs 4B,F and 5B,G,H) giving to the cytoplasm a vacuolated appearance. Ribosomes were mainly concentrated around the endoplasmic reticulum (Fig. 5D,H). The Golgi apparatus was also well represented and showed typical stacks of flatterned cisternae, vescicles and vacuoles, some of which were very large (Fig. 5E–H). Finally, electron microscopy indicated that the irregularities of the plasma membrane seen by light microscopy were due to small pseudopodia located all around the cells (Figs 3 and 4E,F,H).

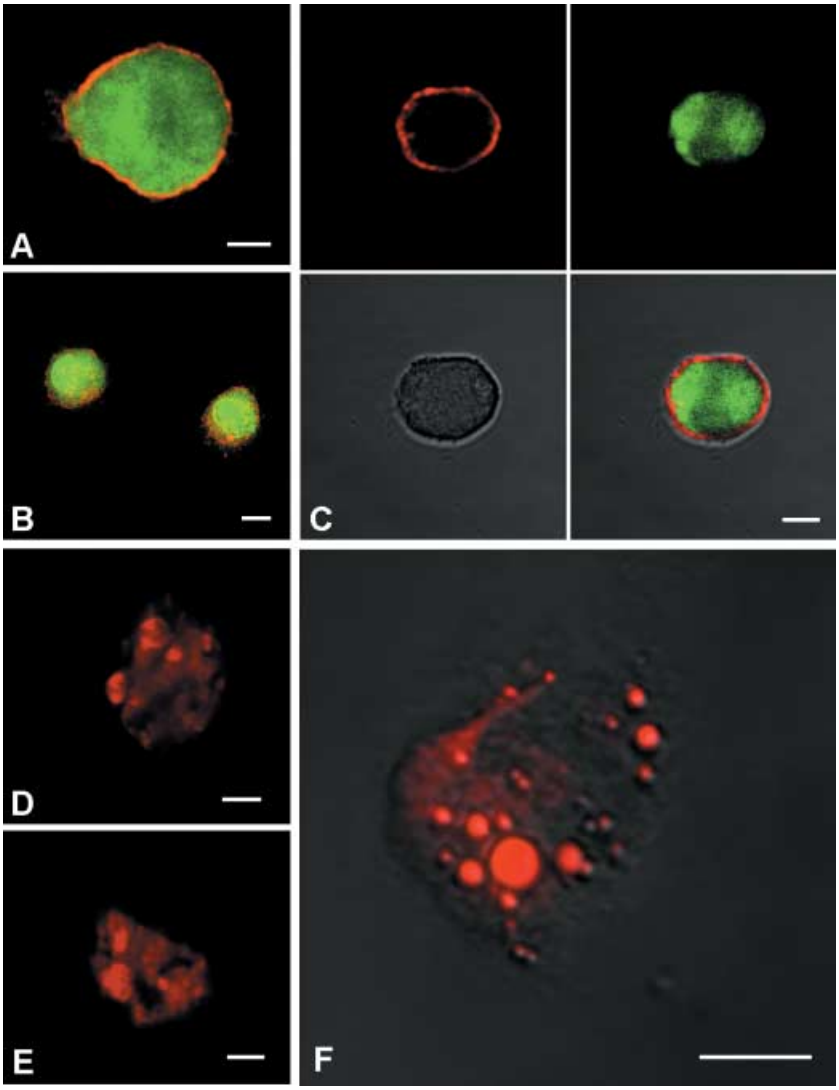

Fig. 1 Confocal laser imaging of GFP-positive (green) mesenchymal stem cells in suspension labelled with CD90 (red) stem cell marker (A–C). MSCs differentiated in adipocytes labelled with Nile Red, a selective fluorescent stain for the detection of intracellular lipid droplets (D–F). Scale bars, 10 μm.

Structural and ultrastructural observations on MSCs harvested from control untransfected animals (data not shown) revealed no morphological differences from those obtained from transfected animals, except for the green autofluorescence.

Discussion

The possibility of transplanting autologous adult stem cells into damaged organs has opened prospects for treating severe human diseases such as acute myocardial infarction (Orlic et al. 2002; Lee et al. 2004; Pittenger & Martin, 2004). Among the various possible sources of such cells, MSCs have been studied extensively because of their ability to self-renew and to give rise to a variety of differentiated cell types (Pittenger et al. 1999; Javazon et al. 2001; Barry & Murphy, 2004; Lovell & Mathur, 2004) and because of the relative ease with which they can be obtained from bone biopsies and cultured.

Here we describe the morphology of cultured MSCs harvested from the bone marrow of GFP stably transfected adult rats. To the best of our knowledge, this is the first comprehensive morphological analysis of these cells using light, confocal and electron microscopy. Although our study focused mainly on MSCs of transfected animals, observations on MSCs harvested from normal adult rats showed that, apart from the green autofluorescence, cell morphology was not modified by GFP expression. This is novel finding given that, despite the increasing use of GFP for labelling stem cells, no study has yet determined whether the presence of the GFP gene modifies cell ultrastructure.

We have isolated MSCs from rat bone marrow and characterized this cell population. To be certain that

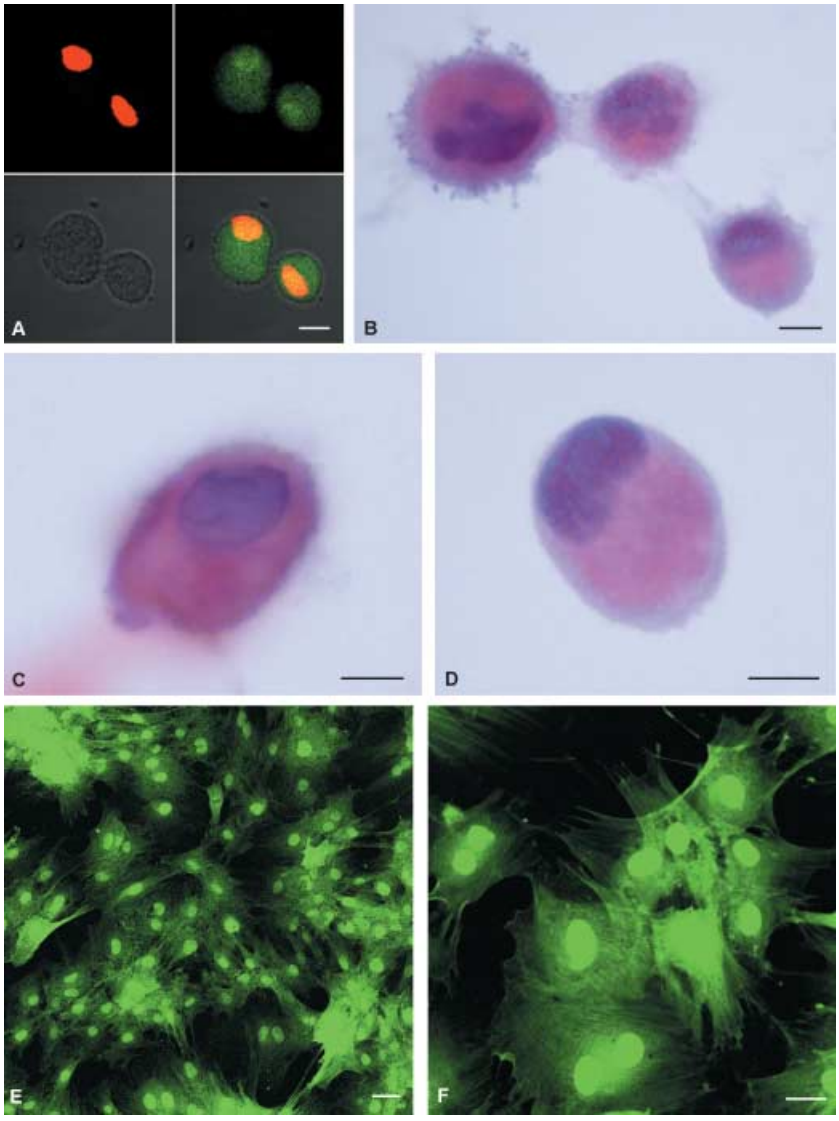

Fig. 2 Confocal laser imaging of GFP-positive mesenchymal stem cells in suspension. All cultured mesenchymal stem cells show strong green autofluorescence. MSCs are also labelled with propidium iodide (red), a nuclear marker (A). Light micrographs of mesenchymal stem cells in suspension stained with haematoxylin and eosin (B–D). The cells have an eccentric nucleus and the cytoplasm is divided into two differently stained areas: a more intensely stained inner zone and a thin peripheral zone with a pale appearance. The plasma membrane showed an irregular profile. GFP-positive adherent cells (E,F) show a central, round nucleus and an irregular cytoplasm profile due to the presence of adherence pseudopodia. Scale bars, 10 μm.

we have separated this particular cell population, we have used an isolation technique that is considered to be specific for separating MSCs (Friedenstein et al. 1976; Javazon et al. 2001; Barry & Murphy, 2004; Muscari et al. 2005). In addition, we showed that all cells were CD90-positive and CD34-negative (Pittenger et al. 1999; Colter et al. 2000). However, it has been suggested that $CD90^+$ and $CD34^-$ may not be enough to ascertain the mesenchymal origin of cells (Javazon et al. 2004). For this reason, we carried out a differentiation experiment and showed that, under appropriate culturing conditions (Rim et al. 2005), many cells acquired an adipocyte phenotype, a property that is presently considered a critical requirement in identifying a putative MSC population (Javazon et al. 2004).

Regarding the protocol for isolating MSCs, we used the traditional technique originally described by Friedenstein in 1976 and which has been repeated by many other authors (e.g. Barry & Murphy, 2004; Strawn et al. 2004; Muscari et al. 2005). This technique allows a sufficient amount of cells to be obtained easily and in a reasonable amount of time (few weeks). However, other effective techniques for MSC isolation can be used, including plating at low density (Prockop et al. 2001), plating in columns (Gronthos et al. 2003) and culturing for long periods of time (Jiang et al. 2002).

Although MSCs are a heterogeneous population in respect to the expression of immunocytochemical markers (Javazon et al. 2004; Young & Black, 2004), the morphological observations reported in the present paper show that the MSC population is relatively

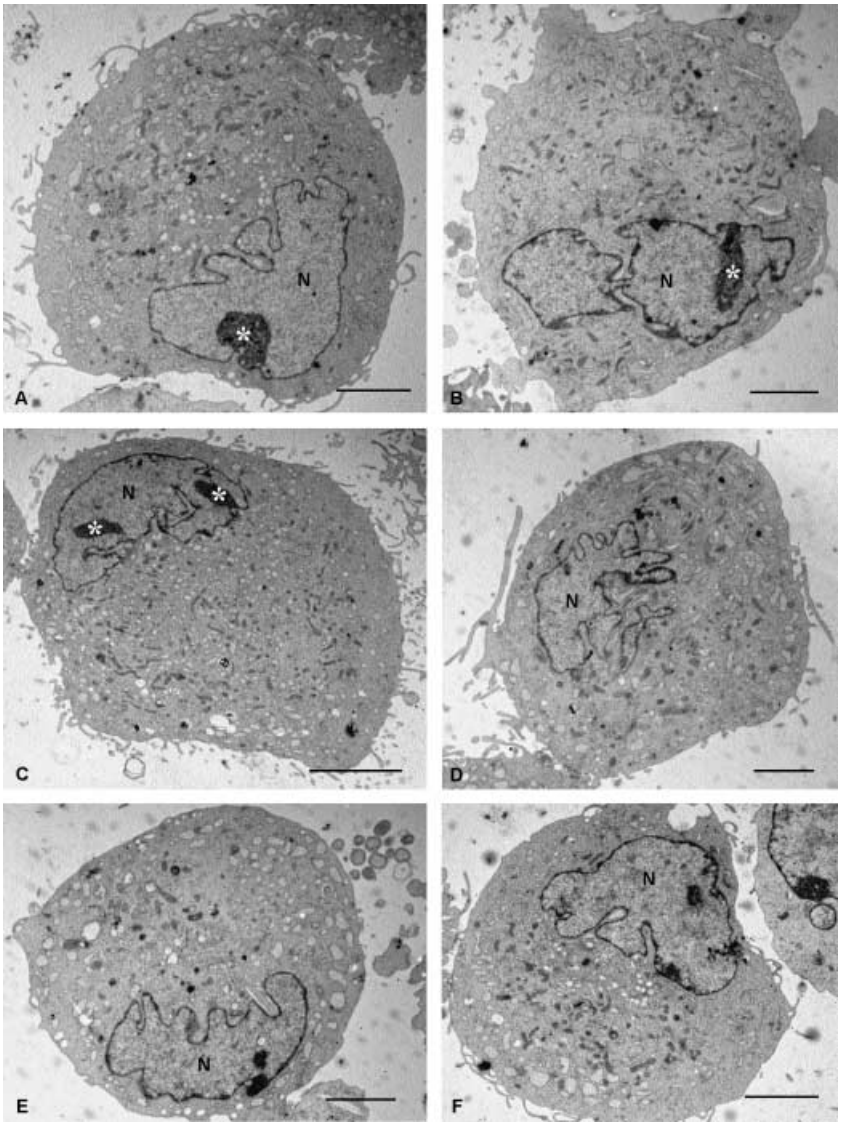

Fig. 3 Electron microscopic images of MSCs cut near the equatorial level. All cells show similar morphological features: an eccentric and irregularly shaped nucleus (N), usually with multiple nucleoli (asterisks), a rich granular endoplasmic reticulum and many mitochondrial profiles. Scale bars, 5 μm.

uniform, especially in terms of ultrastructure. This observation might be particularly useful for detecting them after they are injected into other tissues and for describing the modifications they undergo after transplantation. With this goal in mind, this study focused on suspended MSCs rather then adherent cells because this is the condition in which these cells are transplanted into receiving tissues. However, it should be expected that the *in vivo* environment modifies the phenotype of transplanted cells, and this needs to be taken into consideration, especially in examinations a long time after transplantation.

Among the various morphological features detected, the presence of many small pseudopodia around the entire periphery is interesting because it might help to explain the capacity of the cells for migration within the receiving tissue (Wu et al. 2003; Lee et al. 2004). In addition, electron microscopy revealed two ultrastructural features that distinguish MSCs from fibroblasts: first, the eccentric, irregularly shaped nucleus; and second, the relative richness of the inner cytoplasmic zone in cytoplasmic organelles (especially mitochondria and Golgi apparatus). In general, the ultrastructural appearance of the MSCs indicates that they are stem cells in a relatively advanced state of differentiation.

To our knowledge, there are only four published studies which provide information on the ultrastructure of MSCs (Zohar et al. 1997; Ghilzon et al. 1999; Colter et al. 2001; Prockop et al. 2001). Comparing data from our experiment with those of the first two studies is difficult for two reasons. First, there was only limited electron microscope imaging of their results: a small

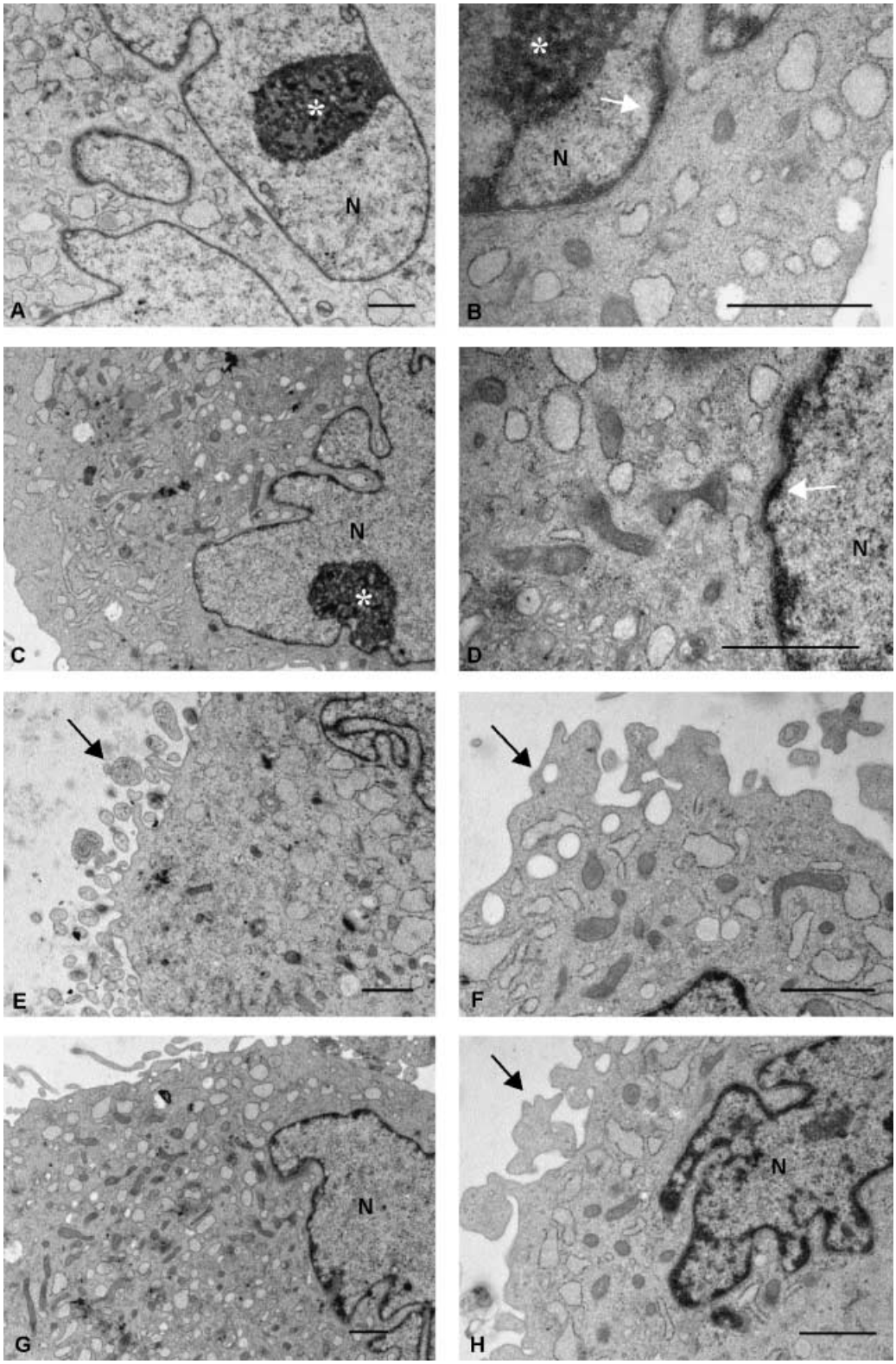

Fig. 4 Electron microscopic images taken at higher magnification show further ultrastructural features of mesenchymal stem cells. Nucleoli (asterisks) are located near the perinuclear cisternae (A–C). Chromatin forms a thin and dense layer inside the perinuclear cisternae (B,D: white arrows). Mitochondrial profiles are denser in the inner part of the cytoplasm (C,E). The plasma membrane has many thin pseudopodia (E–H). Scale bars, 1 μm.

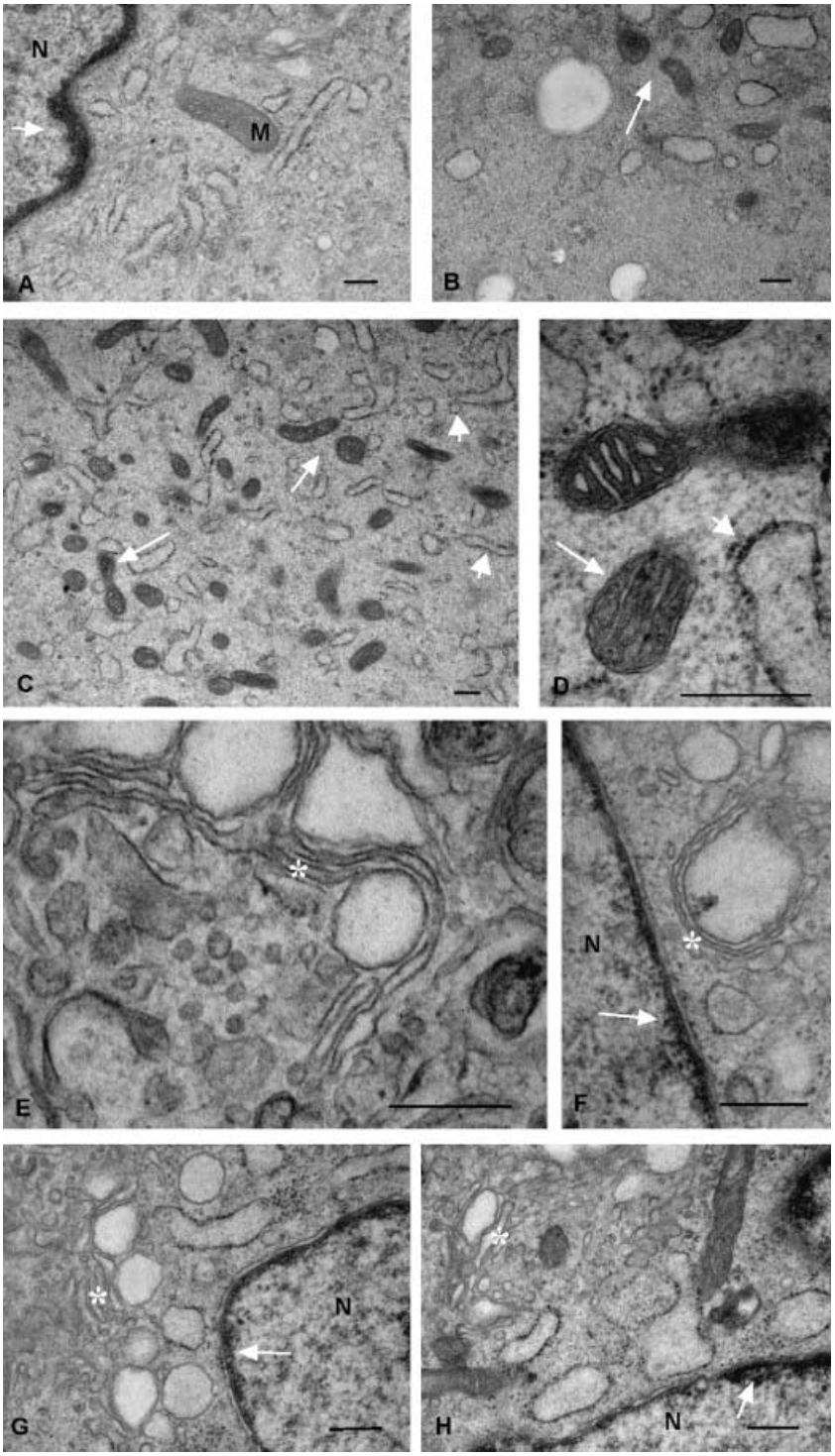

Fig. 5 Other electron microscopic images at high magnification reveal in more detail the ultrastructure of the thin layer of chromatin inside the perinuclear cisternae (A,F,G,H: arrows); the mitochondria, which showed both rounded and elongated profiles and thick cristae (B–D: thin arrows); the granular endoplasmic reticulum organized into small elements (C,D: thick arrows); and the Golgi apparatus, which showed typical stacks of flatterned cisternae, vescicles and vacuoles (E–H: asterisks). Scale bars, 0.5 μm.

number of low-magnification images (Ghilzon et al. 1999) or no image at all (Zohar et al. 1997). Secondly, observations were carried out on cells at day 2 of culturing (P1), whereas our investigation was made at a later stage of differentiation (P6, day 18–24). The latter point explains why these authors reported MSCs of a small size, low granularity and low cytoplasmic/nuclear ratio, which are features of poorly differentiated cells.

The other two papers (Colter et al. 2001; Prockop et al. 2001) provide an ultrastructural description of more mature MSCs (day 15). Both studies reported that MSCs are 'frequently binucleate'; however, our findings

suggest that this observation may have been due to the irregular shape of the nucleus (as illustrated in Fig. 3) and not due to the presence of two nuclei.

Additionally, both studies reported that MSCs 'contained a large number of unidentified vacuoles' in the cytoplasm (Colter et al. 2000, 2001). Our observations suggest that these 'unidentified vacuoles' are in most cases the result of a dilatation of endoplasmic reticulum and Golgi apparatus.

In conclusion, we have provided a comprehensive structural and ultrastructural description of GFP-positive rat MSCs. Our data provide a useful basis for researchers who wish to investigate the differentiation of these cells in normal and pathological tissues. The present study fills a gap existing in the literature regarding a cell population that is attracting a great deal of interest for its potential use as a source of cells for transplantation therapies.

Acknowledgements

We are grateful to Professor Gianni Losano for providing us with GFP-stable transfected animals. This study was supported by Compagnia di San Paolo, Regione Piemonte, University of Turin (ex-60% fund) and MIUR (Cofin fund and FIRB fund). We wish to thank BIOMEDES (Aberdeen, UK) and Jennifer Marie Lee for English language revisions.

References

Abbott JD, Giordano FJ (2003) Stem cells and cardiovascular disease. *J Nucl Cardiol* **10**, 403–412.

Barry FP, Murphy JM (2004) Mesenchymal stem cells: clinical applications and biological characterization. *Int J Biochem Cell Biol* **36**, 568–584.

Colter DC, Class R, DiGirolamo CM, Prockop DJ (2000) Rapid expansion of recycling stem cells in culture of plastic-adherent cells from human bone marrow. *Proc Natl Acad Sci USA* **97**, 3213–3218.

Colter DC, Sekiya I, Prockop DJ (2001) Identification of a subpopulation of rapidly self-renewing and multipotential adult stem cells in colonies of human marrow stromal cells. *Proc Natl Acad Sci USA* **98**, 7841–7845.

Dunnett SB, Bjorklund A, Lindvall O (2001) Cell therapy in Parkinson's disease – stop or go? *Nat Rev Neurosci* **2**, 365–369.

Eisenberg LM, Eisenberg CA (2004) Adult stem cells and their cardiac potential. *Anat Rec Part A* **276A**, 103–112.

Friedenstein AJ, Deriglasova UF, Kulagina NN, et al. (1974) Precursors for fibroblasts in different populations of hematopoietic cells as detected by the in vitro colony assay method. *Exp Hematol* **2**, 83–92.

Friedenstein AJ, Gorskaja U, Kalugina NN (1976) Fibroblast precursors in normal and irradiated mouse hematopoietic organs. *Exp Hematol* **4**, 267–274.

Gerecht-nir S, Fishman B, Itskovitz-Eldor J (2004) Cardiovascular potential of embryonic stem cells. *Anat Rec Part A* **276A**, 58–65.

Geuna S, Borrione P, Fornaro M, Giacobini-Robecchi MG (2001) Adult stem cells and neurogenesis: historical roots and state of the art. *Anat Rec* **265**, 132–141.

Ghilzon R, McCulloch CAG, Zohar R (1999) Stromal mesenchymal progenitor cells. *Leukemia Lymphoma* **32**, 211–221.

Greenspan P, Mayer EP, Fowler SD (1985) Nile red: a selective fluorescent stain for intracellular lipid droplets. *J Cell Biol* **100**, 965–973.

Gronthos S, Zannettino AC, Hay SJ, et al. (2003) Molecular and cellular characterisation of highly purified stromal stem cells derived from human bone marrow. *J Cell Sci* **116**, 1827–1835.

Hassink RJ, de la Rivière AB, Mummery CL, Doevendans PA (2003) Transplantation of cells for cardiac repair. *J Am Coll Cardiol* **41**, 711–717.

Henningson CT Jr, Stanislaus MA, Gewirtz MA (2003) 28. Embryonic and adult stem cell therapy. *J Allergy Clin Immunol* **111**, S745–S753.

Herzog EL, Chai L, Krause DS (2003) Plasticity of marrow-derived stem cells. *Blood* **102**, 3483–3493.

Javazon EH, Colter DC, Schwarz EJ, Prockop DJ (2001) Rat marrow stromal cells are more sensitive to plating density, and expand more rapidly from single-cell-derived colonies than human marrow stromal cells. *Stem Cell* **19**, 219–225.

Javazon EH, Beggs KJ, Flake AW (2004) Mesenchymal stem cells: paradoxes of passaging. *Exp Hematol* **32**, 414–425.

Jiang Y, Vaessen B, Lenvik T, Blackstad M, Reyes M, Verfaillie CM (2002) Multipotent progenitor cells can be isolated from postnatal murine bone marrow, muscle, and brain. *Exp Hematol* **30**, 896–904.

Kicic A, Shen WY, Wilson AS, Constable IJ, Robertson T, Rakoczy PE (2003) Differentiation of marrow stromal cells into photoreceptors in the rat eye. *J Neurosci* **23**, 7742–7749.

Lee MS, Lill M, Makkar RR (2004) Stem cell transplantation in myocardial infarction. *Rev Cardiovasc Med* **5**, 82–98.

Lewis JP, Trobaugh FE Jr (1964) Haematopoietic stem cells. *Nature* **204**, 589–590.

Lovell MJ, Mathur A (2004) The role of stem cells for treatment of cardiovascular disease. *Cell Prolif* **37**, 67–87.

Muscari C, Bonafè F, Stanic I, et al. (2005) Polyamine depletion reduces TNF (alpha) /MG132-induced apoptosis in bone marrow stromal cells. *Stem Cells* **23**, 983–991.

Okabe M, Ikawa M, Kominami K, Nakanishi T, Nishimune Y (1997) 'Green mice' as a source of ubiquitous green cells. *FEBS* **407**, 313–319.

Orlic D, Kajstura J, Chimenti S, et al. (2001) Bone marrow cells regenerate infarcted myocardium. *Nature* **410**, 701–705.

Orlic D, Hill JM, Arai AE (2002) Stem cells for myocardial regeneration. *Circ Res* **91**, 1092–1102.

Pittenger MF, Mackay AM, Beck SC, et al. (1999) Multilineage potential of adult human mesenchymal stem cells. *Science* **284**, 143–147.

Pittenger MF, Martin BJ (2004) Mesenchymal stem cells and their potential as cardiac therapeutics. *Circ Res* **95**, 9–20.

Prockop DJ, Sekiya I, Colter DC (2001) Isolation and characterization of rapidly self-renewing stem cells from cultures of human marrow stromal cells. *Cytotherapy* **3**, 393–396.

Rim JS, Mynatt RL, Gawronska-Kozak B (2005) Mesenchymal stem cells from the outer ear: a novel adult stem cell model system for the study of adipogenesis. *FASEB* **19**, 1205–1207.

Strawn WB, Richmond RS, Ann Tallant E, Gallagher PE, Ferrario CM (2004) Renin–angiotensin system expression in rat bone marrow haematopoietic and stromal cells. *Br J Haematol* **126**, 120–126.

Wezeman FH, Gong Z (2004) Adipogenic effect of alcohol on human bone marrow-derived mesenchymal stem cells. *Alcohol Clin Exp Res* **28**, 1091–1101.

Wu GD, Nolta JA, Jin YS, Barr ML, Yu H, Starnes VA, et al. (2003) Migration of mesenchymal stem cells to heart allografts during chronic rejection. *Transplantation* **75**, 679–685.

Young HE, Black AC Jr (2004) Adult stem cells. *Anat Rec Part A* **276A**, 75–102.

Zohar R, Sodek J, McCulloch CA (1997) Characterization of stromal progenitor cells enriched by flow cytometry. *Blood* **90**, 3471–3481.